18TH WORLD CONFERENCE ON EARTHQUAKE ENGINEERING
WCEE2024
MILAN

MILAN, ITALY
30TH JUNE - 5TH JULY 2024
www.wcee2024.it

THE SHEAR STRAIN INDEX TO TRACK THE SOIL NONLINEARITY IN THE ITALIAN SEISMIC CONTEXT

G. Falcone[1], A. Chiaradonna[2], A. Mendicelli[3], G. Acunzo[4] & M. Moscatelli[3]

[1] University of Napoli Federico II, Naples, Italy, gaetano.falcone@unina.it

[2] University of L'Aquila, L'Aquila, Italy

[3] National Research Council, Monterotondo (Rome), Italy

[4] Theta Group, Rome, Italy

Abstract: *Site response analysis plays a crucial role in seismic hazard assessment and the design of earthquake-resistant structures. While equivalent-linear approaches have been widely adopted due to their simplicity, recent studies have highlighted their limitations when peak shear strains exceed 0.4% for periods less than 0.5 s. This discrepancy between equivalent-linear and non-linear analyses can be better understood through the application of the shear strain index (i.e., the ratio of input motion peak velocity to time-averaged shear-wave velocity in the top 30 m of the soil profile), an innovative parameter that has been successfully employed in North America but remains unexplored in the context of Italian seismicity. This study aims to investigate the effectiveness of the shear strain index in some areas of Italy with different level of seismic hazard, where significant soil nonlinearity is expected. By conducting equivalent linear and non-linear dynamic analyses on well-investigated sites, the maximum shear strains obtained from the analyses will be compared against the predictions derived from an independent application of the shear strain index. The research methodology involves selecting representative sites in Italy and conducting comprehensive geotechnical investigations. Equivalent linear and non-linear dynamic analyses will be performed, considering a range of input ground motions with varying characteristics. The resulting shear strains obtained from the analyses will then be compared to the shear strain index predictions to evaluate their agreement and identify potential discrepancies. The findings of this study will provide valuable insights into the applicability of the shear strain index in the Italian context. Furthermore, they will serve as a critical step towards the classification of the Italian territory into different risk groups, enabling the identification of high-hazard areas where non-linear dynamic analyses should be mandatory. The outcomes of this research will contribute to advancing site response analysis practices in Italy and aid in refining seismic hazard assessments. By addressing the limitations of equivalent linear approaches and exploring the potential of the shear strain index, engineers and researchers can improve the accuracy of seismic design and strengthen the resilience of infrastructure in high-risk areas.*

1. Introduction

Following the February 2023 earthquakes that affected Turkey and Syria, the international communities experienced once again the devastation induced by strong seismic events and realized the importance of adequate investments in the assessment of the seismic risk. In this framework, the site effects were determined to be a crucial role in several strong earthquakes in both Italy, e.g., San Giuliano di Puglia in 2002 (Puglia et al., 2009) and worldwide, e.g., Mexico City in 1985 (Seed et al., 1988).

The site effects are assessed through Site Response Analyses (SRA) able to predict the ground surface motion. This latter is used to design/solve problems at the scale of the single structure, and to support studies at a large scale such as the third-level seismic microzonation (Moscatelli et al., 2020).

The importance of performing SRAs has been recognized also by the national building code, which prescribed the execution of SRA every time the subsoil conditions are not classified in one of the categories reported in table 3.2.II (NTC 2018).

The SRA can be performed according to two main approaches (Chiaradonna, 2022): the pioneering method approximates the actual nonlinear hysteretic stress-strain behavior of cyclically loaded soils by equivalent linear soil properties. This philosophy is implemented in the 'Equivalent Linear' (EQL) codes which operate in the frequency domain through Transfer Functions. Afterward, 'Non-Linear' (NL) methods solve the ground motion equations in the time domain (Kwok et al., 2007). The use of equivalent linear methods is realistic for low and medium cyclic strains, γ, while the use of non-linear methods is preferable in the higher strain range (Kaklamanos et al., 2013, 2015; Régnier et al., 2018). As a result, the EQL methods are not always reliable.

Kim et al. (2016) investigated the conditions for which NL SRA results are distinct from EQL results and provide guidance for predicting when differences are large enough to be of practical significance. EQL/NL differences resulted dependent on an innovative index, called 'shear strain index', I_γ, which is defined as the ratio of input motion Peak Ground Velocity (PGV) to time-averaged shear-wave velocity in the top 30 m of the soil profile, V_{s30}. The same authors found a straightforward relationship between I_γ and γ induced by strong earthquakes in the active crustal and stable continental regions of North America. Generally, for small I_γ (generally < 0.03%), EL and NL results are practically identical, whereas, at larger strains, differences can be significant.

Until now, this index was never applied to the context of Italian seismicity. It is also important to mention that all the microzonation studies performed in Italy were performed according to an EQL approach, so methods able to track the soil non-linearity have been never used.

The proposed study aims to test shear strain index on the Italian territory with a preliminary application to four representative well-characterized sites. The following section 2 describes the reference site and the geotechnical model used in the numerical simulations as well as the constitutive models and numerical platforms adopted. The same geotechnical models were reproduced in both the EQL and NL simulations to highlight the differences in the obtained results, expressed in terms of Peak Ground Acceleration (PGA) predicted at the ground level. The adopted computer codes for the analyses are STRATA (Kottke et al., 2018) and PLAXIS 2D (Brinkgreve et al., 2022), for the EQL and NL approaches, respectively. Preliminary findings from the discussion of the results are summarised in the conclusions.

2. Material and methods

Figure 1 show the location of four sites, denotated as 3, 6, 32, and 36, and selected for SRAs from the seismic microzonation studies database (DPC, 2018). The stack of lithotypes and the shear wave velocity profile, $V_S(z)$, for each site are shown in Figure 2. Figure 3 and Figure 4 display the normalized shear modulus $G(\gamma)/G_0$ and damping ratio $D(\gamma)$ curves for cover soils (i.e., clay, sand and gravel) and geological bedrock, respectively. Since no specific laboratory data were available for the considered sites, literature curves were adopted for the three main soil types, i.e., clay, sand and gravel, identified from the lithological description. Linear visco-elastic behaviour was assumed for the seismic bedrock, characterised by a unit weight of 22 kN/m^3 and a damping ratio D = 0.1%. When the V_S of the deepest layer in the lithotypes stack was at most equal to 800 m/s, the shear wave velocity of the seismic bedrock was 800 m/s. Otherwise, when the V_S of the deepest layer in the lithotypes stack exceeded 800 m/s, the shear wave velocity of the seismic bedrock was considered to be equal to the V_S of that deepest layer.

Key parameters, i.e., the depth of the seismic bedrock below the ground surface, H_{800}, V_{S30}, and the time-averaged shear-wave velocity until the bedrock depth, V_{SH}, of the selected sites are listed in Table 1. Values of PGV from Italian reference seismic hazard (Stucchi et al., 2011) for a return period of 475 years are also provided in the same table and denoted PGV_{ref}. Additionally, PGV values for the selected input motions for the SRAs are included in the same table and denoted from PGV_{IM_1} to PGV_{IM_4}. Pseudo-acceleration response and Fourier spectra are presented in Figure 5. A set of 4 signals was selected as outcropping input motions for LSSR analyses of each site. These sets are listed in Table 2.

The PGV_{IM} values were adopted to determine the Shear Strain Index (SSI) as suggested by (Kim et al., 2016) according to Equation (1), calculated as PGV over the V_{S30} in percentage. Furthermore, SSI was based on Equation (2), considering V_{SH} rather than V_{S30}. The obtained indexes are named SSI and SSI_{VSH}, respectively for Equation (1) and (2). All the computed values are listed in Table 3.

Figure 1. Location of the selected sites.

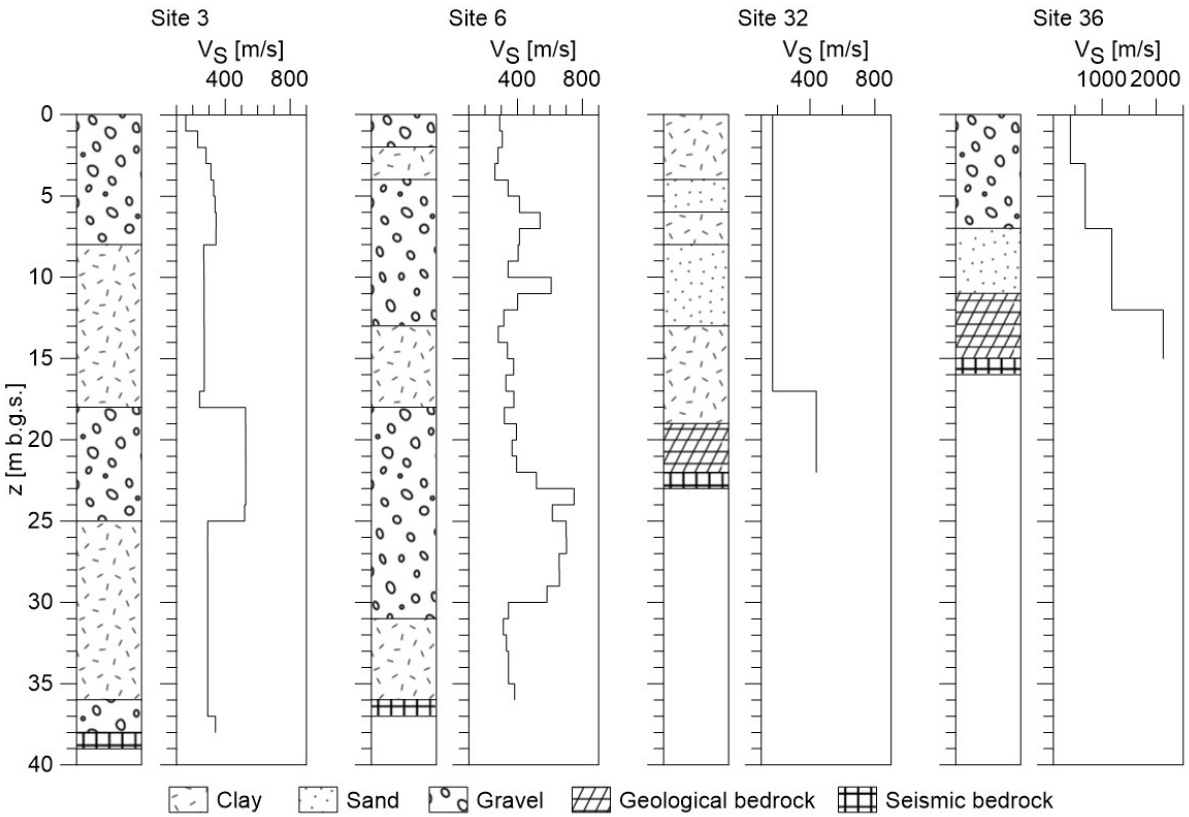

Figure 2. Lithotypes successions and V_S(z) profiles of the selected sites: a) 3, b) 6, c) 32 and d) 36.

One-dimensional total stress dynamic analyses were performed with the computer codes, STRATA and PLAXIS, according to the EQL and NL approaches, respectively.

Strata performs EQL SRA in the frequency domain, using input time series. It is an open-source code, and it has a user-friendly interface. Both peculiarities are among the main reasons for its great popularity. In the case of STRATA, the definition of the geometric scheme is reduced to the identification of the deformable soil (i.e., depth of the seismic bedrock) and the discretization of the soil column in a finite number of sublayers. The maximum thickness of each sublayer is derived from the application of the Kuhlemeyer and Lysmer (1973) criterion.

PLAXIS is a 2D Finite Element (FE) program, developed for the analysis of deformation, stability, and groundwater flow in geotechnical engineering. This commercial code is also quite popular in the professional practice. In this second case, the analysis domain is discretized in triangular elements. The size of the mesh in the wave propagation direction should respect the criterion proposed by Kuhlemeyer and Lysmer (1973). The numerical simulations involved initiating the stress state using the gravity loading option and introducing a subsequent dynamic phase where seismic input motions were applied at the base of the numerical model. The numerical model accounted for the water table at its base and assumed drained conditions for simplicity. In the static stages, standard boundary conditions were applied - specifically, no horizontal displacement was allowed along the vertical sides, and the base of the model had completely fixed displacements. For the dynamic phase, tied degrees of freedom boundary conditions were used along the vertical sides, and a compliant base was employed at the model's bottom. The compliant base condition facilitated the propagation of reference signals, recorded at the outcropping bedrock, as input motions applied at the base of the FE model. On the other hand, the tied degrees of freedom connected nodes at the same elevation on the left and right boundaries, ensuring the simulation of one-dimensional wave propagation. This setup effectively enabled the one-dimensional vertical propagation of shear waves during the dynamic simulations, utilizing a time step equivalent to that of the input signals.

If in STRATA the shear modulus reduction and damping ratio curves are provided point by point, in PLAXIS the constitutive model Hardening Soil Small-Strain (Di Lernia et al., 2019; Schanz et al., 1999) was adopted to model the considered literature curves. Moreover, a small amount of Rayleigh damping, equal to 0.01% and associated to the two frequencies of 1 and 10 Hz, has been introduced in the dynamic analyses to avoid zero dissipation at very low strain levels.

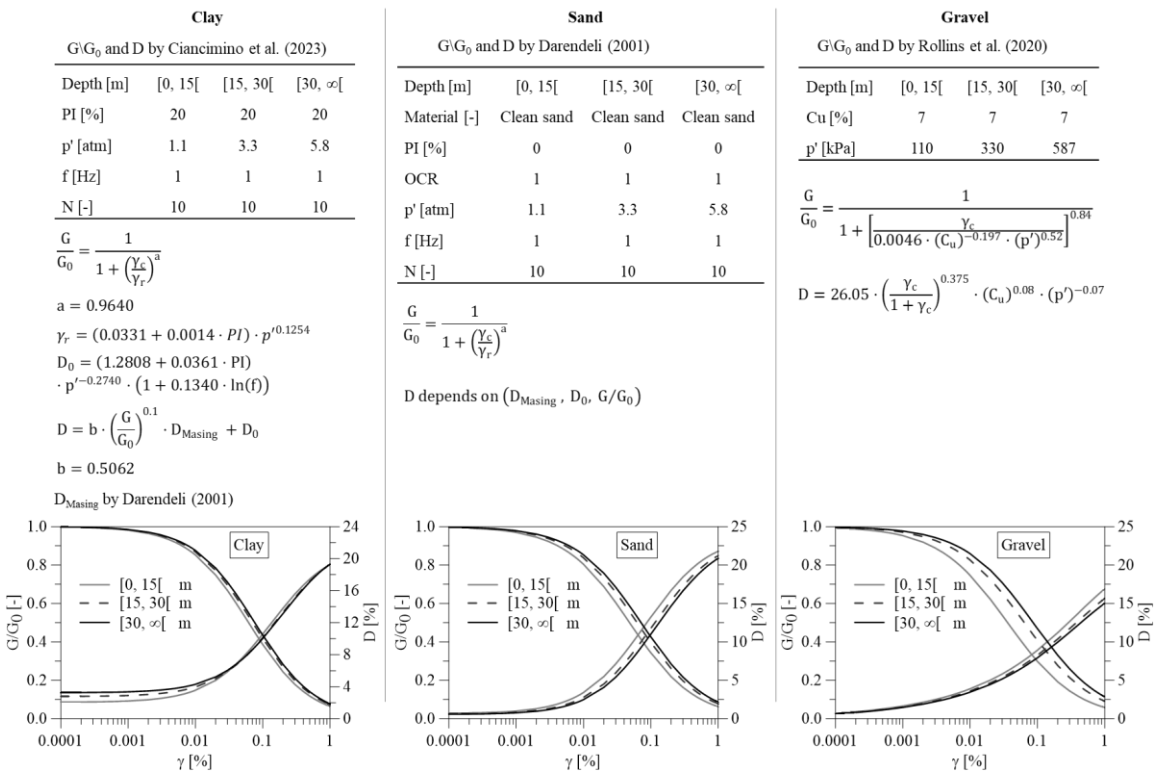

Figure 3. G(γ)/G₀ and D(γ) curves for covers (Ciancimino et al., 2023; Darendeli, 2001; Rollins et al., 2020).

Depth [m]	[0, ∞[
Material [-]	Clay
PI [%]	200
OCR [-]	1
p' [atm]	5.8
f [Hz]	1
N [-]	10

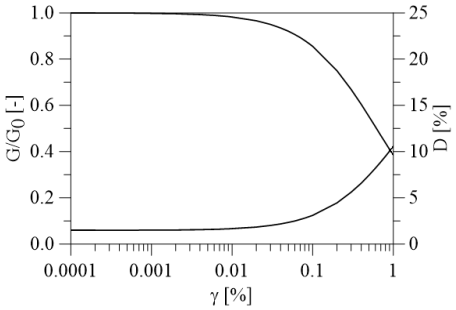

Figure 4. $G(\gamma)/G_0$ and $D(\gamma)$ curves for geological bedrock (Darendeli, 2001).

Table 1. Key parameters of selected sites and input motions.

Site	H_{800}	V_{S30}	V_{SH}	PGV_{ref}	PGV_{IM_1}	PGV_{IM_2}	PGV_{IM_3}	PGV_{IM_4}
[-]	[m b.g.s.]	[m/s]	[m/s]	[m/s]	[m/s]	[m/s]	[m/s]	[m/s]
3	38	309	306	0.109	0.094	0.130	0.110	0.091
6	36	401	390	0.110	0.078	0.130	0.110	0.091
32	22	247	198	0.110	0.095	0.120	0.110	0.103
36	12	1167	695	0.127	0.078	0.167	0.130	0.094

$$\mathrm{SSI} = \frac{\mathrm{PGV}}{\mathrm{V_{S30}}} \tag{1}$$

$$\mathrm{SSI_{V_{SH}}} = \frac{\mathrm{PGV}}{\mathrm{V_{SH}}} \tag{2}$$

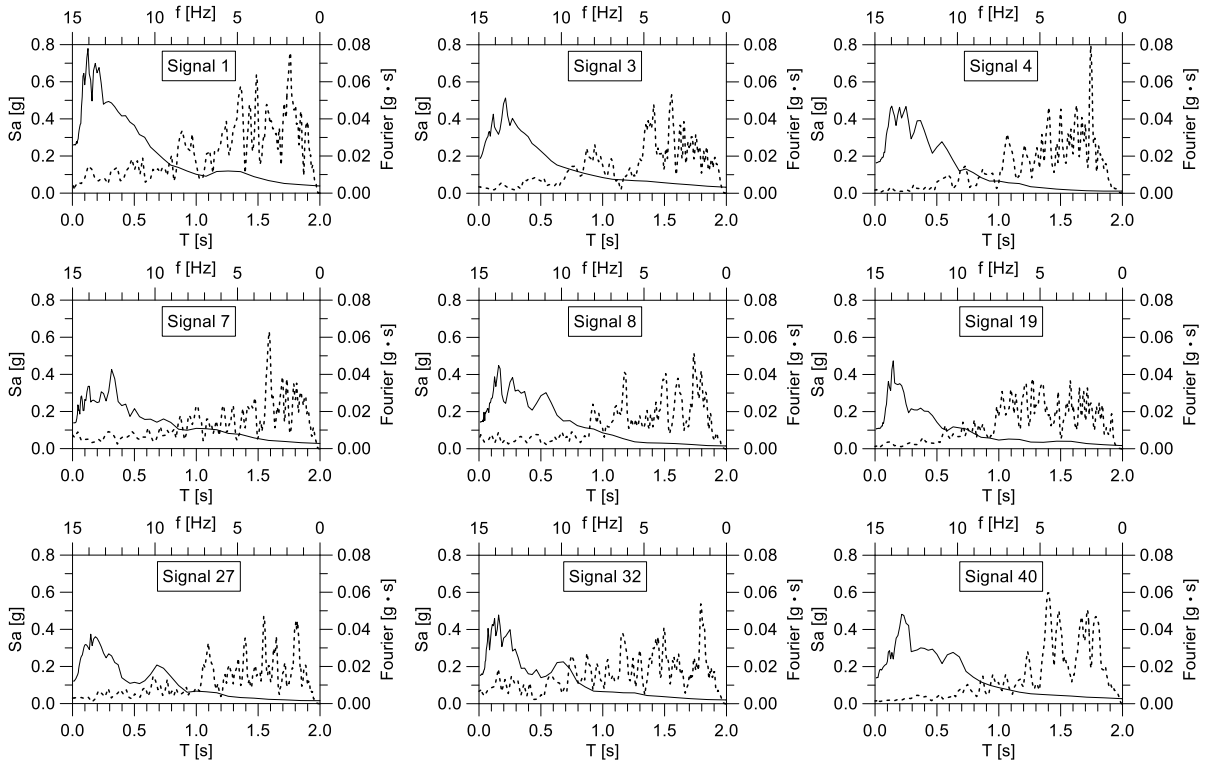

Figure 5. Pseudo-acceleration response (continuous lines) and Fourier (dashed lines) spectra of the input motions.

Table 2. Association between selected reference signals and the input motion ID for LSSR analyses.

Site	IM_1	IM_2	IM_3	IM_4
3	32	3	4	8
6	19	3	4	8
32	27	40	4	7
36	19	1	3	32

Table 3. SSI values for the selected case studies considering both reference hazard (PGV_{ref}) and input motion (IM) selected for LSSR analyses.

Site	SSI_{ref}	SSI_{IM_1}	SSI_{IM_2}	SSI_{IM_3}	SSI_{IM_4}	SSI_{VSH_ref}	$SSI_{VSH\_IM\_1}$	$SSI_{VSH\_IM\_2}$	$SSI_{VSH\_IM\_3}$	$SSI_{VSH\_IM\_4}$
[-]	[%]	[%]	[%]	[%]	[%]	[%]	[%]	[%]	[%]	[%]
3	0.035	0.030	0.042	0.035	0.029	0.036	0.031	0.042	0.036	0.030
6	0.027	0.020	0.032	0.027	0.023	0.028	0.020	0.033	0.028	0.023
32	0.044	0.038	0.049	0.044	0.042	0.055	0.048	0.061	0.055	0.052
36	0.011	0.007	0.014	0.011	0.008	0.018	0.011	0.024	0.019	0.014

3. Results

Comparison between EQL and NL results is presented in terms of profiles of PGA with depth and PGA error (∆PGA), quantified using Equation (3) for each depth of interest. Initially, ∆PGA at the ground surface (i.e., for z = 0) is listed in Table 1. Overall, EQL results are 20% lower than NL results, except for site 32, where EQL PGAs (z = 0) are consistently higher than NL results for each selected input motion.

Figure 6 shows the PGA(z) profiles. EQL results closely resemble NL results for Site 36, which is characterized by the lowest H_{800}, regardless of the input motion. For other sites, EQL PGA is either higher or lower than NL results depending on the input motion. Generally, the greater the thickness of the deposit, the greater the depths affected by EQL results differing from the NL ones. To better illustrate the effect of the depth to the seismic bedrock (i.e., H_{800}) and the deposit stiffness (i.e., V_{S30}), Figure 7a and b display scatter plots of the ∆PGA errors with respect to H_{800} and V_{S30}, respectively. Overall, higher H_{800} and V_{S30} values correspond to lower ΔPGA and reduced error variability.

$$\Delta\mathrm{PGA} = \frac{\mathrm{PGA_{EQL}} - \mathrm{PGA_{NL}}}{\mathrm{PGA_{NL}}} \cdot 100 \qquad (3)$$

Table 4. ∆PGA referred to the comparison of EQL and NL results at the ground surface.

Input / Site	1	2	3	4
3	-17.0	-8.4	-6.5	-1.0
6	29.4	-5.9	9.2	-7.9
32	6.4	31.0	8.0	23.6
36	-5.9	-4.3	-2.3	-8.2

The box plots of ∆PGA considering SSI and SSI_{VSH} are presented in Figure 8a and b, respectively. Specifically, the box plots in Figure 8a confirm the SSI ranges suggested by (Kaklamanos et al., 2013; Kim et al., 2016):

the median value and variability (represented by the grey box indicating the distance between the 25th and 75th percentiles of the ΔPGA distribution) close to 0 correspond to SSI values lower than 0.025%, while for SSI greater than 0.025%, there is a higher variability in ΔPGA, with median ΔPGA values oscillating around 0, taking on both positive and negative values. Additionally, the median values of ΔPGA are consistently lower than 20% for the selected case studies. It is important to note that case studies with SSI higher than 0.09%, for which NL analyses are recommended according to (Kaklamanos et al., 2013; Kim et al., 2016), are not included here for brevity. Furthermore, Figure 8b, displaying the box plots of ΔPGA considering SSI_{VSH}, clearly illustrates the following: EQL results closely resemble NL results for SSI_{VSH} lower than 0.025%, EQL results are generally lower than NL results (ΔPGA lower than 0) for SSI_{VSH} in the range of 0.025%–0.050%, and EQL results are generally higher than NL results (ΔPGA higher than 0) for SSI_{VSH} higher than 0.050%.

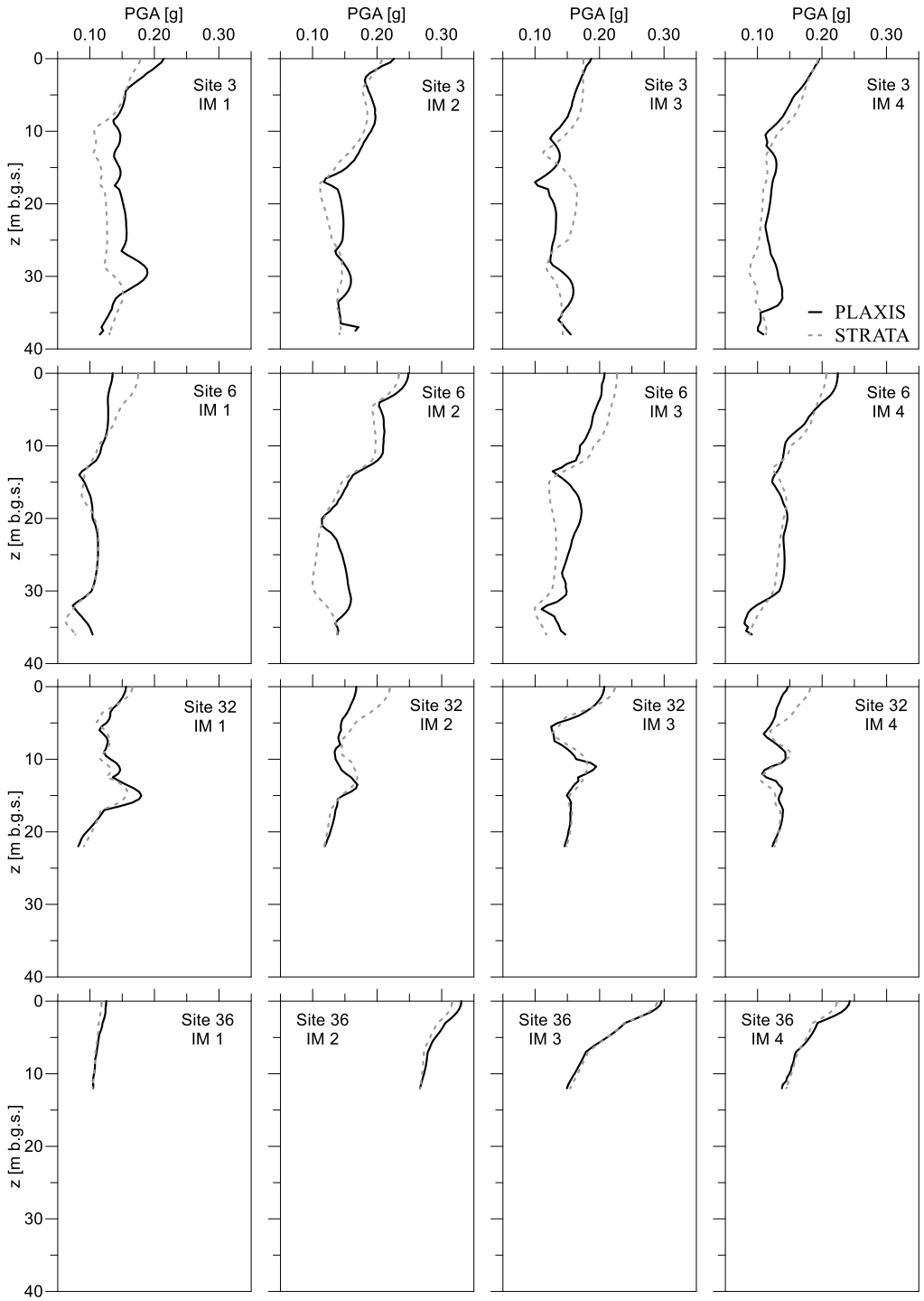

Figure 6. PGA profiles with depth based on EQL (STRATA) and NL (PLAXIS) analyses.

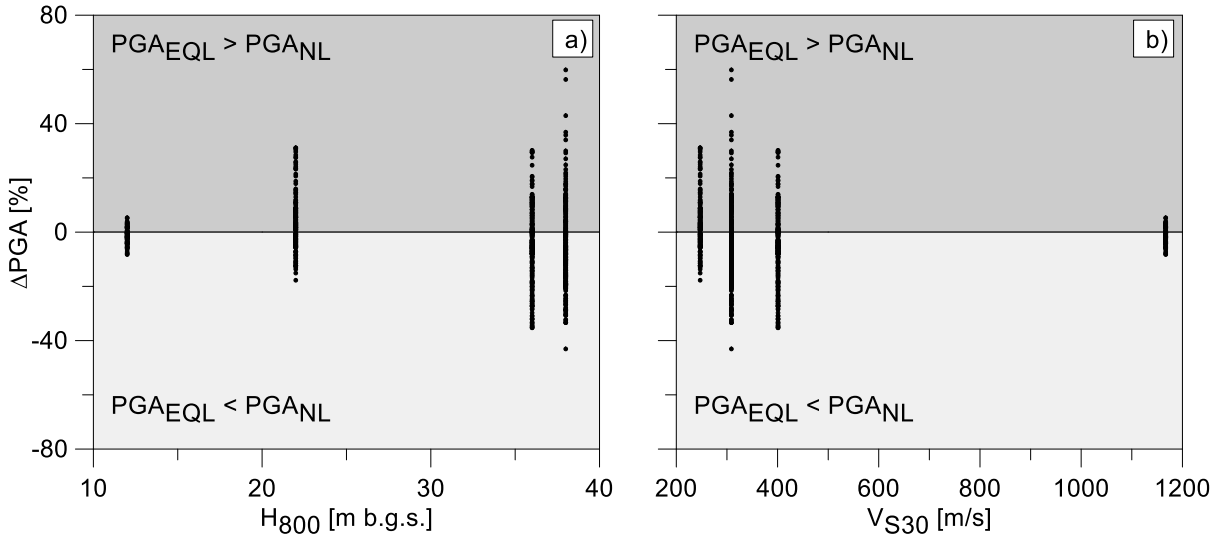

Figure 7. Scatter plots of ΔPGA errors with respect to a) H_{800} and b) V_{S30}.

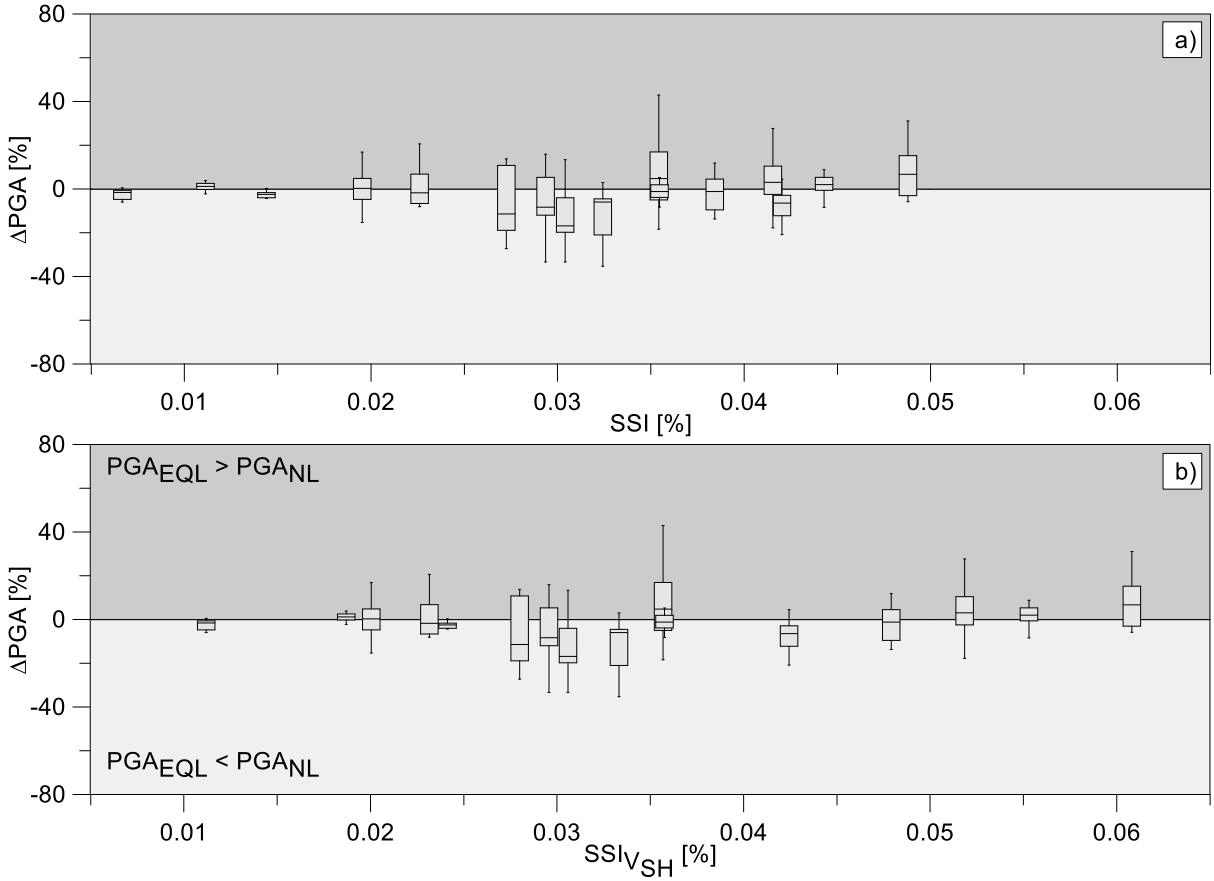

Figure 8. Box plots of ΔPGA errors considering a) SSI and b) modified SSI named SSI_{VSH} in the figure.

4. Conclusions

Local seismic site response analyses were performed for 4 Italian sites adopting both equivalent linear, EQL, and non-linear, NL, approaches. Four input motions were selected and applied as the outcrop motion. The shear strain index was calculated as peak ground velocity, PGV, over the mean shear wave velocity in the upper 30 m of the deposit in percentage and as PGV over the mean shear wave velocity from the ground surface down to the seismic bedrock expressed as a percentage and was denoted SSI and SSI_{VSH}, respectively. The computed SSI ranges from 0.007% to 0.049%, while SSI_{VSH} from 0.011% to 0.061%. It was

proved that for the Italian selected sites characterised by SSI lower than 0.025%, the results from EQL analyses are similar to those from NL analysis. Considering SSI exceeding 0.025% high variability of EQL results was observed with respect to the NL ones with both underestimation and overestimation cases. Furthermore, considering SSI_{VSH} it is possible to recognise three zone of performance on EQL analyses when compared to NL ones: EQL results closely resemble NL results for SSI_{VSH} lower than 0.025%, EQL results are generally lower than NL results (DPGA lower than 0) for SSI_{VSH} in the range of 0.025%–0.050%, and EQL results are generally higher than NL results (DPGA higher than 0) for SSI_{VSH} higher than 0.050%.

Thus, SSI was proved to be a good indicator of the EQL performance over large areas aimed at recognising sites where EQL results are acceptable and those areas where NL analyses are required. Moreover, the SSI_{VSH} could be a better parameter for describing the performance of EQL analyses still remaining the limitation that maps of mean shear wave velocity from the ground surface down to the seismic bedrock are not available everywhere, while maps showing the mean shear wave velocity in the upper 30 m are wide diffuse in the globe.

Future research should consider cases characterized by values of SSI, SSI_{VSH}, and depth to the seismic bedrock higher than the maximum values adopted in this study. This will allow for an evaluation of the performance of the EQL approach in various site conditions, particularly in scenarios where EQL results are expected to significantly differ from those of NL.

Additionally, these preliminary findings did not consider the variability of the NL results when different codes and constitutive models are adopted, which can be also quite important (Régnier et al., 2018). More than one NL code for seismic response analyses will be also considered in the future.

The findings of the study will be used to classify the Italian territory into different groups and identify a priority list of high-risk areas, where NL analyses are necessary.

5. Acknowledgments

This study is part of the project: “ASSIST: Application of the Shear Strain Index as Screening criteria to Track the soil non-linearity” funded by the University of L’Aquila through the call ‘Progetti di Ateneo per la ricerca di base e avvio alla ricerca - anno 2023’.

This research was partially supported by the Italian Department for Civil Protection of the Presidency of Council of Ministers within the “Contratto concernente l’affidamento di servizi per il programma per il supporto al rafforzamento della Governance in materia di riduzione del rischio sismico e vulcanico ai fini di protezione civile nell’ambito del PON Governance e Capacità Istituzionale 2014–2020 - CIG6980737E65” and by European Union - Next Generation EU, in the framework of the GRINS - Growing Resilient, INclusive and Sustainable project (GRINS PE00000018 - CUP E63C22002140007). The views and opinions expressed are solely those of the authors and do not necessarily reflect those of the European Union, nor can the European Union be held responsible for them.

6. References

Brinkgreve, R.B.J., Kumarswamy, S., Swolfs, W.M., 2022. PLAXIS 2D CONNECT Edition V22 Update 1.

Chiaradonna A (2022) Defining the Boundary Conditions for Seismic Response Analysis—A Practical Review of Some Widely-Used Codes. Geosciences 12(2). MDPI: 83.

Ciancimino, A., Cosentini, R.M., Foti, S., Lanzo, G., Pagliaroli, A., Pallara, O., 2023. The PoliTO–UniRoma1 database of cyclic and dynamic laboratory tests: assessment of empirical predictive models. Bulletin of Earthquake Engineering. https://doi.org/10.1007/S10518-022-01573-Y

Darendeli, M.B., 2001. Development of a new family of normalized modulus reduction and material damping curves.

Di Lernia, A., Amorosi, A., Boldini, D., 2019. A multi-directional numerical approach for the seismic ground response and dynamic soil-structure interaction analyses, in: Earthquake Geotechnical Engineering for Protection and Development of Environment and Constructions- Proceedings of the 7th International Conference on Earthquake Geotechnical Engineering, 2019. pp. 2145–2152.

DPC, 2018. Commissione tecnica per il supporto e monitoraggio degli studi di Microzonazione Sismica [WWW Document]. URL www.webms.it (accessed 10.21.22).

Kaklamanos, J., Bradley, B.A., Thompson, E.M., Baise, L.G., 2013. Critical Parameters Affecting Bias and Variability in Site‐Response Analyses Using KiK‐net Downhole Array Data. Bulletin of the Seismological Society of America 103, 1733‐1749. https://doi.org/10.1785/0120120166

Kaklamanos J, Baise LG, Thompson EM, et al. (2015) Comparison of 1D linear, equivalent-linear, and nonlinear site response models at six KiK-net validation sites. Soil Dynamics and Earthquake Engineering 69. Elsevier: 207–219. DOI: 10.1016/J.SOILDYN.2014.10.016.

Kim, B., Hashash, Y.M.A., Stewart, J.P., Rathje, E.M., Harmon, J.A., Musgrove, M.I., Campbell, K.W., Silva, W.J., 2016. Relative Differences between Nonlinear and Equivalent-Linear 1-D Site Response Analyses. Earthquake Spectra 32, 1845–1865. https://doi.org/10.1193/051215EQS068M

Kottke AR, Wang X and Rathje EM (2018) Strata Technical Manual. Available at: https://github.com/arkottke/strata/blob/master/manual/manual.pdf.

Kuhlemeyer R.L., Lysmer J. (1973). Finite element method accuracy for wave propagation problems. Journal of the Soil Mechanics and Foundations Division, 99(5), 421-427.

Kwok AOL, Stewart JP, Hashash YMA, et al. (2007) Use of exact solutions of wave propagation problems to guide implementation of nonlinear seismic ground response analysis procedures. Journal of Geotechnical and Geoenvironmental Engineering 133(11). American Society of Civil Engineers: 1385–1398.

Moscatelli M, Albarello D, Scarascia Mugnozza G, et al. (2020) The Italian approach to seismic microzonation. Bulletin of Earthquake Engineering 18(12).

NTC (2018). D.M. 17/01/2018. Aggiornamento delle «Norme Tecniche per le Costruzioni». Gazzetta Ufficiale, n.42 del 20/02/2018 – supplemento ordinario n.8. Ministry of Infrastructure and Transportation.

Puglia R, Klin P, Pagliaroli A, et al. (2009) Analisi della risposta sismica locale a San Giuliano di Puglia con modelli 1D, 2D e 3D. Rivista Italiana di Geotecnica-Italian Geotechnical Journal. Pàtron.

Régnier J, Bonilla LF, Bard PY, et al. (2018) Prenolin: International benchmark on 1D nonlinear: Site-response analysis—validation phase exercise. Bulletin of the Seismological Society of America 108(2). DOI: 10.1785/0120170210.

Rollins, K.M., Singh, M., Roy, J., 2020. Simplified Equations for Shear-Modulus Degradation and Damping of Gravels. Journal of Geotechnical and Geoenvironmental Engineering 146, 04020076. https://doi.org/10.1061/(ASCE)GT.1943-5606.0002300

Seed HB, Romo MP, Sun JI, et al. (1988) The Mexico earthquake of September 19, 1985—Relationships between soil conditions and earthquake ground motions. Earthquake spectra 4(4). SAGE Publications Sage UK: London, England: 687–729.

Schanz, T., Vermeer, P.A., Bonnier, P.G., 1999. The hardening soil model: Formulation and verification. Beyond 2000 in computational geotechnics. Ten Years of PLAXIS International. Proceedings of the international symposium, Amsterdam, March 1999. 281–296. https://doi.org/10.1201/9781315138206-27/HARDENING-SOIL-MODEL-FORMULATION-VERIFICATION-SCHANZ-VERMEER-BONNIER.

Stucchi, M., Meletti, C., Montaldo, V., Crowley, H., Calvi, G.M., Boschi, E., 2011. Seismic Hazard Assessment (2003–2009) for the Italian Building Code. Bulletin of the Seismological Society of America 101, 1885–1911. https://doi.org/10.1785/0120100130